EPJ Web of Conferences **40**, 01003 (2013)
DOI: 10.1051/epjconf/20134001003

Measurement of the Structural Unit in magnetic dispersions

T. Mercer[1, 2] and P.R. Bissell[1, 2]

[1]Jeremiah Horrocks Institute for Mathematics, Physics & Astrophysics, University of Central Lancashire, Preston PR1 2HE, UK
[2]Centre for Materials Science, University of Central Lancashire, Preston PR1 2HE, UK

Abstract. Measurement of the Structural Unit (SU – containing both the solid phase and trapped-fluid within their associated structures) in magnetic dispersions has been carried out using Hindered Settling (HS) analysis that uses scanning column magnetometry and cone & plate rheology techniques. From this, an equivalent Stokes' particle diameter, d, of ($5.2 \leq d \leq 8.2$) microns was determined that is approximately 22 times larger than the iron oxide particles of our formulation. A previous computer simulation based on HS theory produces complete concentration-height profiles of the sedimenting system over time that compare well when using a correspondingly large trapped-liquid fraction of around the 84% of the SU volume determined here, giving confidence in the result. As interest in iron oxide suspensions for potential biomedical and chemical decontamination/catalysis applications continues to grow an understanding of their structures is likely to become increasingly important.

1 Introduction

Interest in magnetic dispersions is well established and wide ranging, arising out of the industrial/engineering applications typically associated with ferrofluids through to the fabrication of advanced flexible recording media [1]. More recently there has been increasing interest in dispersions of magnetic nanoparticles for their potential bio-medical applications [2] such as in drug delivery, contrasting agents and magnetic hyperthermia and hence the development of methods for the characterisation of magnetic dispersions is an important field of study.

In general it is known that suspensions are often complex and cannot be characterised in terms of the microstructure (single particles) alone, but instead consist of Structural Units (SUs) involving multi-particle structures that contain trapped fluid [3]. These associations are formed as particles tend to aggregate into mesostructures of small flocs or clusters, which may in-turn aggregate into larger clusters of clusters. Indeed, if the Pigment/Particle Volume Concentration (PVC) is high enough and the inter-SU bonds strong enough then these SUs may form a network or macrostructure that spans the whole sample and resists sedimentation.

Earlier studies have shown that it is possible to go beyond simple stability measurements and determine the fraction of trapped fluid within the SUs. In the work reported here, this methodology is extended to include a full hindered settling analysis of a sedimenting magnetic suspension of γ-Fe_2O_3 particles from which the size of an equivalent Stokes' particle diameter is determined. The relevance of this to some potential applications, alongside that of the trapped fluid, is also discussed

2 Experimental details

A well-established and stable γ-Fe_2O_3 formulation, based on a commercial preparation used to produce recording media in the form of a 300 Oe back-up/archive tape, was used as our model system. Development of this measurement technique on a well-known system provides the baseline needed for future planned work. Particles from the same batch of given mean length 300 nm and aspect ratio 5:1 were used throughout to produce dispersions 'in-house' using standard premixing and bead milling techniques. Although full details of the formulation are proprietary, it can be stated that the particles coated in surfactant were suspended in a 'free-fluid' phase consisting of a solution of two resins dissolved in an organic solvent.

For the premixing, a DISPERMAT® water-cooled chamber and saw-tooth blade were used. Milling and letdown were carried out in a DISPERMAT® SL-C bead mill using ~ 1mm diameter zirconia beads.

The hindered settling analysis described herein is reliant upon the observation of the dispersion's sedimentation under gravity and of the rheological characterisation of the liquid phase using scanning column magnetometry and cone & plate techniques respectively:

2.1 Scanning column magnetometry

Profiles of particle concentration were obtained using an 'in-house' Scanning Column Magnetometer (SCM). Here the sample tube filled with dispersion is held vertical and is driven down through the otherwise empty core of a coil by a computer controlled stepper motor. This coil forms the inductive part of a tuned circuit wired up in a Colpitts configuration. The resulting signal frequency from the oscillator is determined by an interface box before being fed back to the computer.

The introduction of magnetic material into the coil core causes its inductance to change which results in a corresponding shift in oscillator frequency. The computer compares this frequency with the initial 'sample-free' frequency of 1 Mhz and logs the difference, ΔF, over the column height. It can be shown that this frequency shift is directly proportional to the pigment concentration and so a plot of ΔF as a function of dispersion height provides a particle concentration profile of the whole settling system. The resonant current in the coil produced a maximum peak field of < 0.3 Oe within the sample during measurement.

2.2 Cone & plate rheology

Rheological characterisation of the free-fluid was carried out using a rotational Bohlin CVO controlled stress rheometer with truncated cone and plate geometry CP 4/40 (40 mm diameter cone, 4° cone angle). The automated gap setting procedure of the CVO allowed a consistent cone-to-plate gap of (150 + 1) μm to be set on a daily basis, where 150 μm is the truncation height of the 4° cone. A solvent trap cover was used to minimise evaporation loss and, unless otherwise stated, the temperature was set and controlled at (20.0 + 0.1) °C

Using this set-up allowed two methods of stress viscometry (flow characterisation) and stress sweep oscillation (viscoelastic characterisation) to be carried out as detailed in the results section.

3 Results and discussion

3.1. Observation of hindered settling

SCM plots of magnetic particle concentration as a function of suspension column height can be seen in figure 1. Cumulative plots of the same sample over time are shown in order to illustrate the settling process. The sharp interface of time zero at the top of the column is maintained as gravity sedimentation commences, which is expected in a hindered settling system where a 'plug' of constant PVC falls 'en-bloc' at a constant rate, Q. For more dilute systems (nominal *effective* PVC < 10%), the particles fall as if they are single Stokes particles in an infinite fluid which leads to a dilution of the top interface as particles fall at different rates in accordance with their size distribution. In these *effectively* more concentrated systems (due to trapped fluid that is discussed later) the fall of any one particle is *hindered* by the presence of surrounding neighbours and hence three distinct regions

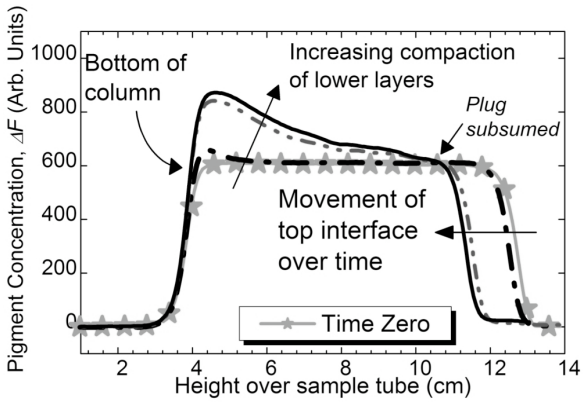

Fig. 1. Typical SCM particle concentration profiles of a suspension of γ-Fe_2O_3 particles. A number of profiles of the same sample are show over approx. 10^3 hours in order to illustrate the sedimenting process. A sharp interface is maintained at the top of the column which is indicative of hindered settling.

form in the column; (i) a *supernatant* of near solids free fluid above (ii) the plug of the *hindered settling* region that falls down into (iii) the *compression zone* of the layers building up at the bottom of the tube. All three of these regions can be clearly seen in figure 1 with the approximate point where the plug has been subsumed indicated. It is at this point that the rate of fall of the top interface (the sludge line) starts to decrease and continues to tail off as the compression increases. In the subsequent hindered settling analysis, it is the initially constant value of Q that is used throughout.

3.2 Rheology measurements

Typical stress viscometry curves as functions of shear rate are shown in figure 2. The viscosity plot is near constant, around a mean value of (169.7 $\pm$ 0.9) mPas, over the full applied shear stress range ($0.06 \leq \sigma \leq 113.7$) Pa. The lower σ point is a consequence of the instrumentation limit and the upper is due to the finding that the fluid would be forced out from under the cone at higher values. The highly Newtonian response is also depicted by the shear stress plot of the same figure. The expected linear correlation through the origin is clearly illustrated by the linear regression. The position of the rise in viscosity, η, at the low (crowded) end of the plot is more easily picked out in the inset, where the same curve is plotted on a semi-log scale. This is due to the logarithmic steps of σ applied by the Bohlin CVO. It can be seen from the inset that the rise is, in fact, an upturn as the shear rate tends to zero, which was always observed in this fluid.

The upturn could be the approach to a 2nd (higher) Newtonian plateau at zero shear that is sometimes observed. On the other hand, a η curve that tends to infinity at zero shear might be expected (if more points below the lower σ limit could be obtained) which is indicative of a yield stress. As a yield stress is the rupture point of any fluid structure, below which no flow will occur, the next set of measurements was concerned with an attempt to characterise this structure by oscillatory means

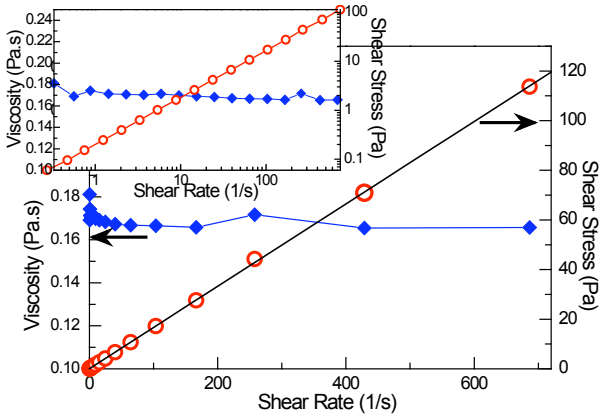

Fig. 2. Typical Stress Viscometry profiles for the free-fluid. The highly linear regression that passes through the origin on the main shear stress plot is expected in a Newtonian liquid. The same plot in the inset, but on a logarithmic scale, allows the position of the rise in viscosity at low shear rates to be more readily picked out

A typical stress sweep oscillation for the free-fluid carried out at 0.5 Hz is shown in figure 3. In this case, a sinusoidal stress of amplitude σ_0 was applied to the fluid and the resultant strain amplitude of γ_0 was measured. From these, the complex modulus G^* may be defined, and found, using $G^*=\sigma_0/\gamma_0$. As there is also a phase shift, ϕ, between the stress and strain waveforms, the complex modulus can be expressed in terms of the elastic modulus G' and the viscous modulus G'', where

$$G^* = G' + iG'' \qquad (1)$$

and so $G' = G^*\cos(\phi)$ and $G'' = G^*\sin(\phi)$ can then be used to quantify these components. As can be seen in figure 3, the linear *increase* in the response of the strain with applied stress defines the Linear Visco-Elastic Region (LVER) within which the viscoelastic structure is intact, i.e. it is *not* being ruptured. Hence the moduli are expected to be independent of the stress and subsequent strain amplitudes when in the LVER, yielding values of the viscoelastic structure for that fluid. This effect can be seen on the same figure in the near constant part of the elastic modulus curve, with a low mean value of $G'=(10 \pm 1)$ mPa, that only begins to change sharply beyond the critical stress, σ_c, value of around 6 Pa of the upper LVER limit as the viscoelastic structure starts to break down. Likewise, the phase shift plot remains flat out to σ_c with a mean value of $\phi=(88.7 \pm 0.1)$ degrees. This indicates a near-Newtonian response, where $\phi=90°$ for a purely viscous fluid at one limit and 0° at the other for an ideal elastic solid. Confirmation of the approach to a pure viscous fluid was provided by the G'' curve (not shown here). Again, the plot was almost constant out to σ_c, with the resultant value of $G''=(434 \pm 1)$ mPa meaning that the fluid is viscous dominated with a G''/G' ratio of 43.

Hindered settling analysis relies on a Stokes-like approach where a particle (or SU assembly of particles) 'feels' a *viscous drag* on its motion as it sediments through a fluid. Given the highly Newtonian flow response of the free-fluid (figure 2), it is reasonable to assume that the viscosity values obtained may be used for quantitative analysis in hindered settling models. More weight is added to this argument when the viscoelastic characteristics are examined (figure 3). Again the fluid is dominated by viscous components and so a near-Newtonian response would be expected. It should be noted that hindered settling has also been observed in some non-Newtonian fluids [4]

3.3 Hindered settling analysis and the determination of SU size

A number of models have been put forward and used successfully in order to describe hindered settling, most notably that of Steinour [5] and Richardson-Zaki [6]. For Steinour, the rate of fall of the hindered settling plug or sludge line, Q, was developed using both a theoretical and empirical approach that resulted in the semi-empirical relationship of

$$Q = V_s \varepsilon^2 10^{-A(1-\varepsilon)}, \qquad (2)$$

where A is usually classed as a system dependant constant, ε is the porosity or void fraction, defined as $\varepsilon = 1\text{-PVC}$, and Stokes' velocity, V_s, is that of an equivalent unhindered spherical particle settling in an infinite fluid (i.e. the point where $Q \to V_s$ as $\varepsilon \to 1$).

The Richardson-Zaki equation was found empirically and is given as

$$Q = V_s \varepsilon^n \qquad (3)$$

Again, n is classed as a system dependant constant with the other terms as described previously. Hence a plot of $\log(Q)$ as a function of $\log(\varepsilon)$ should result in a linear correlation of gradient n and a regression constant of $\log(V_s)$ at the point where $\log(\varepsilon)$ is zero (i.e. an extrapolation to the point where $\varepsilon = 1$ at infinite dilution). This is shown in figure 4, resulting in values of $n = 48$ and $V_s = 7.4 \times 10^{-8}$ ms^{-1}. However, this plot fails to take into account the effects of trapped-fluid within the SU assemblies. Over two articles [5, 7], Steinour developed

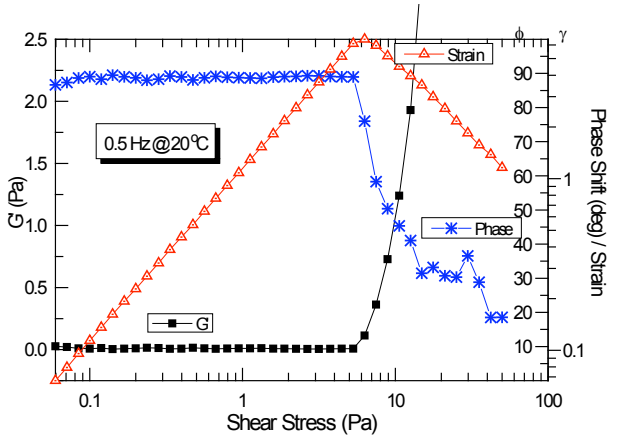

Fig. 3. Stress sweep oscillation plot at 0.5 Hz for the free fluid of the γ-Fe_2O_3 formulation. The near constant G' curve for $\sigma < 6$ Pa defines the LVER, above which the sudden change from increasing to decreasing strain shows the structure is now being broken down. The near-Newtonian response of the fluid is indicated by the near π/2 phase shift over the LVER

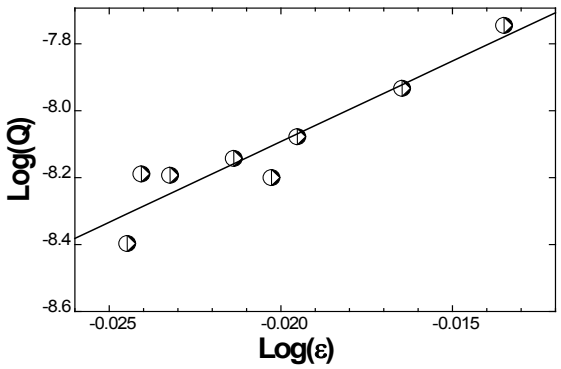

Fig. 4. Hindered settling analysis after the method of Richardson-Zaki [6]. Despite the high degree of scatter, correction for trapped fluid results in model parameters that reduce near to, or agree with, those found in simple systems that contain little-to-no trapped-liquid

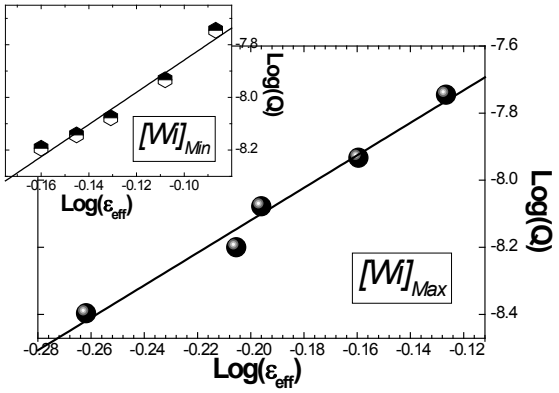

Fig. 5. Richardson-Zaki hindered settling analysis now corrected for the effects of trapped fluid. The main plot and the inset use the data points associated with the upper and lower *Wi* limits respectively.

the concept and determination of the *effective* porosity ε_{eff} of a system. He showed that, unlike his simple experimental model systems (uniform spheres in oil), in real systems a proportion of the liquid becomes trapped within particle assemblies and so is *not* able to flow up and through the settling bed. Hence, this liquid is often termed the *immobile* or *trapped-fluid* and it moves down with the settling solid phase.

Using the Steinour method, the volume ratio of trapped-fluid to the total solids and trapped-fluid, *Wi*, was found to range from 0.83 to 0.88. Full details of this previous work are given elsewhere [8], where confidence in the rather scattered data seen in figure 4 is given by correction of three different hindered settling models to take into account the trapped fluid. In each case the various model parameters reduced to values close to, or in agreement with, the fundamental parameters found originally in the simple model systems that contain little to no trapped-fluid. Further confidence was gained from the large *Wi* values found in our previous computer simulation [9]. A close match with the SCM sedimentation profiles of a similar γ-Fe_2O_3 dispersion was only obtained when the PVC was increased beyond the experimental value of ~ 5% to about 60%. This shift corresponds to an increase in *Wi* from zero to 0.90 that is comparable with our upper *Wi* limit of 0.88. In conjunction with the corrected results, this implies that the *Wi* value obtained from the Steinour analysis is a realistic estimate.

Using the upper and lower limits of *Wi*, it is now possible to carry out a full hindered settling analysis by replacing each ε term in the models by the *effective* porosity given by $\varepsilon_{eff} = (\varepsilon - Wi)/(1 - Wi)$. This is shown in figure 5 after the method of Richardson-Zaki where the main plot and the inset use the same data sets [8] associated with $(Wi)_{MAX}$ and $(Wi)_{MIN}$ respectively. From the linear regressions, values within the *Wi* limits of $(5.66 < V_s < 7.07)$ x 10^{-8} ms^{-1} were determined. Likewise, from the linear correlation of $\log(Q/\varepsilon_{eff}^{\ 2})$ as a function of ε_{eff}, (not shown) the semi-empirical hindered settling model of equation (2) was used to find $(6.79 < V_s < 9.71)$ x 10^{-8} ms^{-1}. Hence, using given values for the particle density; ρ_p, (4700 kgm^{-3}) and the free-fluid density, ρ_f, (963 kgm^{-3}) in conjunction with the η, *Wi* and V_s values determined here, the size of the equivalent Stokes' diameter, *d*, of the SU may be found from Stokes' equation in the form

$$d = \sqrt{\frac{18 V_s \eta}{g\left(\left(\rho_p\right)_{eff} - \rho_f\right)}} \qquad (4)$$

where the *effective* particle density (solid plus trapped fluid) is defined as $(\rho_p)_{\text{eff}} = (1\text{-}Wi)\rho_p + Wi\rho_f$ and *g* is the gravitational constant. From this, the SU size of $(5.2 \leq d \leq 8.2)$ μm was evaluated which at the mid-point of 6.7 μm is approximately 22 times larger than the given length (~ 0.3 μm) of the γ-Fe_2O_3 particles.

The large SU size and its associated trapped fluid could have a significant effect in potential bio-medical applications, where the structures may be subject to an applied field or to the stress of blood flow. As detailed earlier, the SU is likely to be made-up of smaller sub-SUs on different size scales across the meso to micro range. Increasing the shear forces on the suspensions causes a progressive break down of the SU into its sub-SUs, releasing part of the trapped fluid in the process. Localised dilution around the particles may then upset the chemical balance required for any particular process and may need to be considered. The quantitative value for the SU equivalent diameter can also be readily transformed into a volume surface area which would be especially useful for input and comparison with computer simulations of these systems. Further work has now started on an experimental investigation of Superparamagnetic iron oxide nanoparticles (SPIONS) and will be reported in due course.

References

1. J.R. Lin, Tribol. Int., **49**, 110 (2012)
2. T. Sen, *et al*, RSC Advances, **2**, 5221 (2012)
3. D. Quemada, Eur. Phys. J. AP, **1**, 119 (1998)
4. R. Buscall, J.W. Goodwin, R.H. Ottewill and T.F. Tadros, J. Colloid Interface Sci., **85**, 78 (1982)
5. H.H. Steinour, Ind. Eng. Chem., **36**, 840 (1944)
6. J.F. Richardson and W.N. Zaki, Trans. Instn Chem. Engrs., **32**, 35 (1954)
7. H.H. Steinour, Ind. Eng. Chem., **36**, 618 (1944)
8. T. Mercer, P.R. Bissell and R.G. Gilson, IEEE Trans. Magn., **38**, 3219 (2002)
9. T. Mercer, P.R. Bissell, J.A. Gotaas and R.G. Gilson, J. Magn. Magn. Mater., **193**, 284 (1999)